# On-orbit Spatial Resolution Estimation of CBERS-2 Imaging System Using Ideal Edge Target

Kamel Bensebaa, Gerald J. F. Banon, Leila M. G. Fonseca and Guaraci J. Erthal

Image Processing Division - National Institute for Space Research (INPE)
Av. dos Astronautas, 1758, 12227-010 São José dos Campos, Brazil (South America)
phone: 55 12 39 45 65 22, fax: 55 12 39 45 64 68,
{camel, banon, Leila, gaia}@dpi.inpe.br

**Abstract.** The China-Brazil Earth Resources Satellite (CBERS-2) has been developed by China and Brazil and was launched on October 2003. This satellite carries three sensors: WFI, CCD and IRMSS. Due to limitations of the CCD sensor components, the images acquired by the imaging system undergo a blurring. Under the hypothesis that the Point Spread Function (PSF) of the imaging system is Gaussian, the blurring effect of an ideal step edge can be represented as an error function (erf). As the PSF is assumed separable, its identification reduces to the estimation of two standard deviations or equivalently to two EIFOVs (Effective Instantaneous Field of View), one for the along-track direction and another for the across-track. This work describes an approach for the on-orbit CBERS-2 CCD spatial resolution estimation using a set of subimages of natural edges and allows an objective assessment of the imaging system performance.

**Keywords:** CCD camera, spatial resolution, estimation, modelling, measurement, target, erf, edge spread function, point spread function, EIFOV.

## 1 Introduction

A cooperative remote-sensing program between Brazil and China initiated in 1988, has resulted in the development and the building up a set of remote sensing satellites called CBERS (China-Brazil Earth Resources Satellite). These satellites allow monitoring their huge territories, mainly: environmental change, ground survey, natural disaster, agriculture and deforestation.

The first stage of this program was accomplished by the launching of CBERS-1 on October 1999, which operated until August 2003. The second stage of the program consisted of the launching on October 2003 of CBERS-2, technically similar to its predecessor, with only minor changes to ensure its reliability.

Imagery from orbiting sensors has provided much information about the Earth's surface and the effects of human activities upon it. For this information be useful, it is critical to access the imagery system performance. One performance measure is related to the blurring effect due to the instrumental optics (diffraction, aberrations, focusing error) and the movement of the satellite during the imaging process.

Hence, the images may have a blurred appearance that is likely to compromise their visual quality and analysis. In this sense, the performance evaluation of imaging system in term of spatial resolution estimation is an important issue.

In general, the blurring effect is related to the Point Spread Function (PSF) in the spatial domain and to the Modulation Transfer Function (MTF) in the frequency domain [6]. For translation invariant linear system, the PSF characterizes the imaging system. Under the assumption that the PSF is Gaussian and separable, its identification reduces to the estimation of two parameters called EIFOV (Effective Instantaneous Field of View), one for the along-track direction and another for the across-track which are equal to 2.66 times the standard deviation [2], [16]. This estimation allows spatial resolution estimation, and consequently an objective assessment of the imaging system performance. The EIFOV enables a comparison between different sensors.

Among other approaches, the spatial resolution of an imaging system may be obtained from the blurring effect of an ideal step edge. In natural scenes, edges are not always ideal step edges. For that reason, only the "better" edges are selected. When the imaging system is excited by an ideal step edge, the transition from bright to dark defines the edge sharpness and it is used to estimate the spatial resolution.

This transition is represented by the so-called Edge Spread Function (ESF) [12]. Despite the fact that this function is 2D, it can be characterized through a 1D function along the normal of the edge in the case of translation invariant systems. Furthermore, when the system is linear and the PSF is Gaussian, this function is an error function (erf) which is the convolution product of the ideal step edge with a Gaussian function.

The two EIFOV characteristic parameters of the spatial resolution can be theoretically obtained from two ESFs in different directions. In practice more than two ESFs are convenient to get a more precise estimation.

The objective of this work is to use an approach for an on-orbit assessment performance of the CCD camera of CBERS-2 satellite which doesn't depend on any target size measurement. The approach consists of estimating the along-track and across-track EIFOVs using a set of subimages of natural edges extracted from a scene image of Sorriso town in Mato Grosso state (Brazil). Each selected subimage corresponds to a different edge direction.

A standard deviation associated with each subimage was estimated and the spatial resolution estimation of the along-track and across-track was obtained through an ellipse fitting.

The rest of the paper is organized as follows: Section 2 gives a brief overview of the CBERS-2 satellite. Section 3 summarizes four different PSF estimation approaches. Section 4 and Section 5 introduce respectively the target scene of natural edges between different crops or between crops and nude soils, and the data preparation. Section 6 describes the algorithm used in this work for edge detection and edge cross-section extraction, and it presents the edge model. Section 7 introduces the details of the ellipse fitting technique. Finally, the Section 8 discusses the results and gives the conclusion of this work.

## 2  CBERS-2 Overview

CBERS-2 satellite carries on-board a multisensor payload with different spatial resolutions called: WFI (Wide Field Imager), IRMSS (Infrared MSS) and CCD (Charge Coupled Device) camera. In addition, the satellite carries a Space Environment Monitor for detecting high-energy radiation.

The high-resolution CCD Camera device which is the main study of this work, provides images of 4 spectral bands from visible light to near infrared (B1: 0.45~0.52μm; B2: 0.52~0.59μm; B3: 0.63~0.69μm; B4: 0.77~0.89μm) and one panchromatic band (B5: 0.51~0.73μm). It acquires the earth ground scenes by pushbroom scanning, from a 778 km sun-synchronous orbit and provides images of 113 km wide strips with sampling rate of 20 meters at nadir for the multispectral bands.

## 3  PSF Estimation Approaches

Basically, there are four approaches to determine a PSF or a MTF of an imaging system. They are based on experimental methods or in theoretical modelling of the physical processes under study.

The first approach uses the image system specifications to model its spatial response. Fonseca and Mascarenhas [8] and Markham [15] have used this approach to determine the spatial response of the TM sensor (Landsat satellite).

The second approach uses targets with well-defined shape and size as airport runway, bridges, artificial targets, etc. For these targets, Storey [17] has provided a methodology for on-orbit spatial resolution estimation of Landsat-7 ETM+ sensor by using a Causeway Bridge image (Louisiana – USA). Choi and Helder [7] have used airport runway and a tarp placed on the ground for on-orbit MTF measurement of IKONOS satellite sensor. Bensebaa et al. [4] used an image of an artificial black squared target placed in the Gobi desert (China). The CCD spatial response is modelled as 2D Gaussian function which is characterized by two parameters: one in along-track direction and another in across-track. The EIFOV values are then derived from these parameters. Bensebaa et al. [3] also used natural targets such as the Rio-Niterói Bridge over Guanabara Bay (Brazil) and Causeway Bridge to estimate the spatial resolution in the along-track and across-track directions, respectively.

As opposed to the second approach, in the third approach the target size doesn't need to be known since the target consists of an ideal step edge. This approach was already successfully experimented by Luxen and Förstner [14].

The fourth approach consists of adjusting a simulated low resolution image to an image acquired by the sensor under study. According to Storey [17], this method works satisfactorily if the two sets of imagery are acquired at or near the same time or, at least, under similar conditions to avoid the problems associated with temporal variations. This kind of experiment was used to determine the spatial resolution of the CBERS-CCD cameras using a higher spatial resolution image acquired by the SPOT-4 satellite and an image of the same scene acquired by CBERS satellite [5].

The algorithm proposed in this work belongs to the third approach but differently from the work of Luxen and Förstner [14], the point spread function model used here, may be assumed separable since the selected images are raw data whose rows correspond to the CCD chips and columns correspond to the detectors movements both being in orthogonal directions.

## 4   Target Scene

The initial task is the selection of natural edges between different crops or between crops and nude soils. In this sense, the scene of Sorriso town located 270 miles north of Cuiabá, the state capital of Mato Grosso (Brazil) is perfect. Sorriso County now plants above 700,000 acres of soybeans annually. In addition, this region is also a producer of corn and cotton. Figure 1 shows original image of Sorriso region.
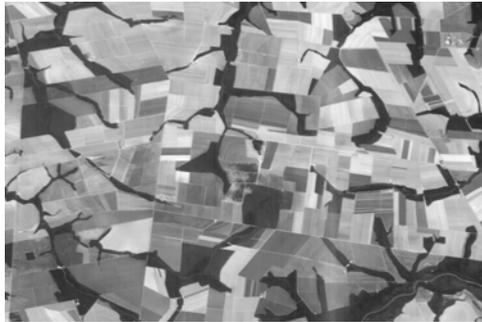


**Fig. 1.** Original image of Sorriso region (band 2).

## 5   Data Preparation

This work used band B2 of the scene of Sorriso with orbit 116 and point 114, acquired on July 15, 2006 by CCD camera on-board CBERS-2. The original cloud free image was a good candidate for the extraction of several subimages of different edge directions. Twelve of these subimages were selected for this work.

## 6   Edge Processing

In this section, we describe the algorithm for edge cross-section extraction as well as the edge model. The illustrations are done, using a subimage with edge direction of 143°.

## 6.1 Edge detection and edge cross-section extraction

The first step of the algorithm is the edge detection. For this step, the Sobel operator [10] was used with a thresholding operation that results in a binary image. This operator was chosen because it's less sensitive to isolated high intensity point. It is a "small bar" detector, rather than a point detector. Figure 2 shows the original subimage and Figure 3 shows the result of Sobel edge operation after thresholding.



**Fig. 2.** Original subimage.



**Fig. 3.** Detected edge.

Once the edge detection operation is performed, its gravity center $G_c$ is computed using the following expression:

$$Gc = \frac{\sum_{(u,v)} (u,v).I_E(u,v)}{\sum_{(u,v)} I_E(u,v)} ,$$ **(1)**

where $(u,v)$ represents the position of each pixel in the binary edge image $I_E$ and $I_E(u,v)$ represents its radiometry.

A $7 \times 7$ subimage was extracted in such a way that its center coincides with the previously computed gravity center. This operation allows the centering of the detected edge in the subimage. Figure 4 shows the centralized subimage and the Figure 5 shows the centralized detected edge.
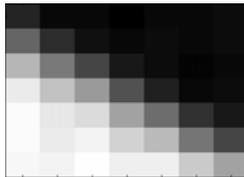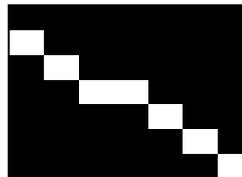


**Fig. 4.** Centralized subimage.



**Fig. 5.** Centralized detected edge.

The parameters *a, b* and *c* of the edge fitting straight line equation:

$$au + bv + c = 0,$$ **(2)**

were estimated by solving the homogeneous linear equation system given by expression:

$$A\boldsymbol{x} = \boldsymbol{0}, \tag{3}$$

where $\boldsymbol{x}$ is the vector of 3 unknowns $\begin{bmatrix} a & b & c \end{bmatrix}^t$, and $\boldsymbol{A}$ is the matrix $M \times 3$ with $M > 3$ given by:

$$A = \begin{bmatrix} u_1 & v_1 & 1 \\ . & . & . \\ u_M & v_M & 1 \end{bmatrix}, \tag{4}$$

where the $(u_i, v_i)_{i=1,..,M}$ are the coordinates of the edge pixels.

The best way to solve Equation (3) is to perform singular value decomposition on the matrix $A$ [13].

The next step consists of extracting the edge cross-section along the edge normal. This edge cross-section is the function $E_R$ that maps the real numbers:

$$\rho(u, v) = \frac{(au + bv + c)}{\sqrt{a^2 + b^2}} \tag{5}$$

to the radiometries $I_R$, when $(u,v)$ runs over the domain of the subimage $I_R$ ($7 \times 7$ set of points). Actually $\rho(u,v)$ represents the distance of the pixels position $(u,v)$ to the edge straight line given by equation (2) [1].

Figure 6 depicts the edge cross-section extracted from a given subimage. The domain unit is meter and the range unit is radiometry digital number.

### 6.2 Edge Model

Let $M_1$ and $M_2$ represent, respectively the least and the greatest values of the edge cross-section, then the edge model is given by:

$$E_M(\rho) = \left(1 - \frac{1}{2} * erfc\left(\frac{\rho - \mu}{\sigma\sqrt{2}}\right)\right) * (M_2 - M_1) + M_1, \tag{6}$$

where *erfc* represents the complementary error function given by:

$$erfc(x) = \frac{2}{\sqrt{\pi}} \int_x^\infty e^{-t^2} dt. \tag{7}$$

In equation (6), the parameters $\mu$ and $\sigma$ represent respectively the mean and the standard deviation of the underlying Gaussian function.

Let RMS($E_R,E_M$) be the root mean square of the difference between $E_R$ and $E_M$:

$$\text{RMS}(E_R, E_M) = \left( \frac{1}{\# Domain(E_R)} \sum \left( E_R - E_M \right)^2 \right)^{1/2} . \tag{8}$$

The estimation procedure has two-steps. At the first step for a given default value $\sigma$, we look for $\mu$ which minimizes RMS($E_R, E_M$). At the second step, we use the previous optimal value $\mu$ and look for $\sigma$ which minimizes RMS($E_R, E_M$). The optimal values have been obtained by nonlinear programming [11].
Figure 7 depicts the result of the fitting of the edge model over the edge cross-section for an edge direction of 143°.
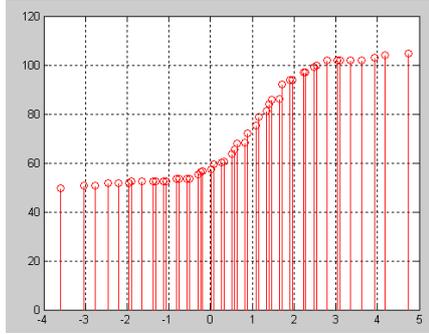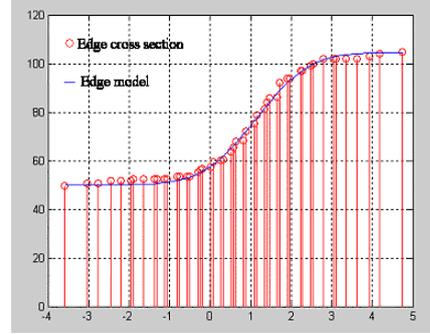


**Fig. 6.** An edge cross-section.



**Fig. 7.** Fitting the edge model over the edge cross-section.

## 7   Ellipse Fitting

The last step is the ellipse fitting. More specifically, because of the separability assumption of the PSF, the problem is the fitting of the ellipse given by the equation [9]:

$$\frac{x^2}{\sigma_x^2} + \frac{y^2}{\sigma_y^2} = 1 \tag{9}$$

over the set of points $(x_i, y_i)$ $i = 1,...,12$ where

$$x_i = \sigma_i \frac{|b_i|}{\sqrt{a_i^2 + b_i^2}} \tag{10}$$

7

$$y_i = \sigma_i \frac{|a_i|}{\sqrt{a_i^2 + b_i^2}} \tag{11}$$

and where $\sigma_i$ is the optimal standard deviation for edge $i$ with parameters $a_i$ and $b_i$. Each point $(x_i, y_i)$ characterizes the blurring effect in the direction of the normal to the edge $i$, its distance to the origin is $\sigma_i$.

The above expression are for an edge direction $arctg(-a_i/b_i)$ comprised between 0 and $\pi/2$. For the other quadrants some appropriate signal must be added in these expressions.

The parameters $\sigma_x$ and $\sigma_y$ are estimated by solving the homogeneous linear equation system given by the following expression:

$$\begin{bmatrix} x_1^2 & y_1^2 & -1 \\ . & . & . \\ x_{12}^2 & y_{12}^2 & -1 \end{bmatrix} \cdot \begin{bmatrix} \alpha \\ \beta \\ \gamma \end{bmatrix} = 0 \ . \tag{12}$$

The estimated values of standard deviations $\sigma_x$ and $\sigma_y$ in along-track and across-track directions are respectively,

$$\sigma_x = \sqrt{\frac{\gamma}{\alpha}} \text{ and } \sigma_y = \sqrt{\frac{\gamma}{\beta}} \ . \tag{13}$$

Finally, the optimal EIFOV values for both directions are related to the standard deviation $\sigma$ by the expression:

$$EIFOV = 2.66.\sigma \ . \tag{14}$$

Results of the optimal values of the standard deviation and the EIFOVs are presented in Table 1. Figure 8 shows the subimages and its corresponding EIFOV while Figure 9 shows the best fitting of the ellipse.

**Table 1**. Results of optimal EIFOVs..

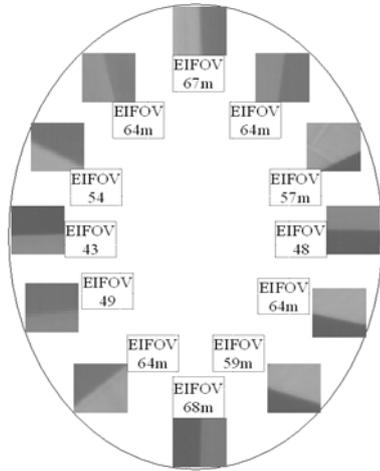| Direction | Estimated Standard Deviation (m) | Estimated EIFOV (m) |
|---|---|---|
| Along-track | 19.2 | 51 |
| Across-track | 25.26 | 67 |

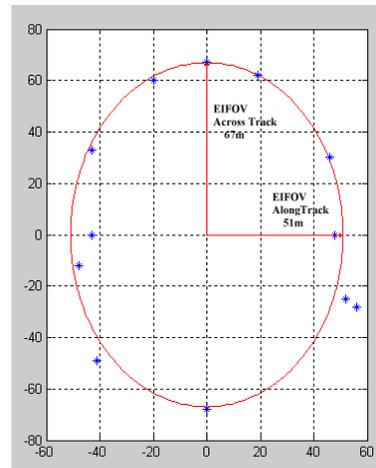**Fig. 8.** Selected subimages.                    **Fig. 9.** Ellipse Fitting.

## 8   Conclusion

In this paper, an approach for CBERS-2 CCD on-orbit spatial resolution estimation has been introduced using subimages of natural edges extracted from the original image of a scene of Sorriso town in Mato Grosso state in Brazil. The results show that the CBERS-2 CCD across-track resolution is worse than the along-track one and confirm the results obtained in previous works. This degradation could be explained by the presence of mirror vibration when both sensors IRMSS and CCD work simultaneously. Besides this hypothesis, the observed degradation could be the result of an electronic coupling between adjacent detectors. In addition, we have noticed a little degradation of the EIFOV in along-track direction in comparison with the previous results [3], [4], [5], even though this method of using edges as targets leads to conservative evaluations because of the difficulty of finding ideal edges. This EIFOV estimation result is valuable in future work on CBERS-2 image restoration.

## References

1. Banon, G. J. F. Bases da computação gráfica. Rio de Janeiro: Editora Campus Ltda, 1989.
2. Banon, G. J. F.; Santos, A. C. Digital filter design for sensor simulation: application to the Brazilian Remote Sensing Satellite. Sao Jose dos campos: INPE, 1993. 62 p. (INPE-5523-RPQ/665). Disponível em:
   <http://bibdigital.sid.inpe.br/rep/dpi.inpe.br/banon/1995/12.14.18.12>. Acesso em: 29 oct. 2003.

3. Bensebaa, K.; Banon, G. J. F.; Fonseca, L. M. G. On-orbit Spatial Resolution Estimation of CBERS-1 CCD Imaging System from bridge images. In: Congress International Society for Photogrammetry and Remote Sensing, 20., 12-23 July 2004, Istanbul, Turkey. Proceedings… Istambul: International Archives of Photogrammetry, Remote Sensing and Spatial Information Sciences, 2004, v. 35, part B1, p. 36-41.

4. Bensebaa, K.; Banon, G. J. F.; Fonseca, L. M. G. On-orbit spatial resolution estimation of CBERS-1 CCD camera. In: International Conference on Image and Graphics (ICIG 2004), 3., 18-20 dec. 2004, Hong Kong, China. Proceedings… Los Alamitos, CA: IEEE Computer Society Press, 2004. v. 2 p. 576-579.

5. Bensebaa, K.; Banon, G. J. F.; Fonseca, L. M. G. On-orbit spatial resolution estimation of CBERS-1 CCD imaging system using higher resolution images. In: Simpósio Brasileiro de Sensoriamento Remoto (SBSR), 12., 2005, Goiânia. Anais… São José dos Campos: INPE, 2005. Artigos, p. 827-834. CD-ROM. ISBN 85-17-00018-8. Disponível em: <http://bibdigital.sid.inpe.br/rep/ltid.inpe.br/sbsr/2004/11.19.19.28>. Acesso em: 12 maio 2005.

6. Bretschneider, T. Blur identification in satellite imagery using image doublets. In: Asian Conference on Remote Sensing, 23., 2002, Kathmandu, Nepal. Proceedings… Kathmandu: GIS Development, 2002, CD-ROM. Disponível em:
< http://www.gisdevelopment.net/aars/acrs/2002/adp/119.pdf > Acesso em: 11 abr. 2004.

7. Choi, T. and  D. Helder. On-Orbit Modulation Transfer Function (MTF) Measurement. Remote Sensing of Environment, v. 88, p. 42.45, 2003.

8. Fonseca, L. M. G.; Mascarenhas, N. D. D. Determinação da função de transferência do sensor TM do satélite Landsat-5. In: Congresso Nacional de Matemática Aplicada e Computacional, 10., 21-26 set. 1987, Gramado, BR. Resumo dos Trabalhos... São José dos Campos: INPE, 1987. p. 297-302. Publicado como: INPE-4213-PRE/1094.

9. Gander, W., Golub, G.H., Strebel, R. Least-squares fitting of circles and ellipses, Bit, 34  (4): 558-578, dec, 1994.

10. Gonzalez, R. C. and Woods, R. E. (1992). Digital Image Processing. Addison-Wesley Publishing Company Inc., 1992.

11. Himmelblau, D. M. Applied nonlinear programming. New York: McGraw- Hill, 1972.

12. Kohm, K. Modulation Transfer Function Measurement Method and Results for The Orbview-3 High Resolution Imaging Satellite. In: Congress International Society for Photogrammetry and Remote Sensing, 20., 12-23 July 2004, Istanbul, Turkey**. Proceedings**… Istambul: International Archives of Photogrammetry, Remote Sensing and Spatial Information Sciences, 2004, v. 35, part B1, p. 7-12.

13. Kreyszig, E. **Advanced engineering mathematics.** New York: John Wiley and Sons, 1993.

14. Luxen, M.; Forstner, W. Characterizing image quality: Blind estimation of the point spread function from a single image. In: ISPRS Commission III Symposium (Photogrammetric Computer Vision), 9-13 Setember 2002, Graz, Austria. **Proceedings**… Graz: PCV02, 2002, v. XXXIV, part 3A, p. 205–210.

15. Markham, B.L. The Landsat sensor's spatial response. **IEEE Transactions on Geoscience and Remote Sensing**, v. 23, n. 6, p. 864-875, nov. 1985.

16. Slater, P.N. **Remote sensing optics and optical system**. London: Addison-Wesley, 1980.

17. Storey, J. C. Landsat 7 on-orbit modulation transfer function estimation. In: Sensors, Systems, and Next Generation Satellites 5., 17-20 sep. 2001, Toulouse, France. **Proceedings**… Bellingham, WA, USA: SPIE, 2001, p. 50-61.